Experimental demonstration of gridless spectrum and time optical switching

N. Amaya,[1,*] G. S. Zervas,[1] M. Irfan,[1] Y. R. Zhou,[2] A. Lord,[2] and D. Simeonidou[1]

[1]*School of Computer Science and Electronic Engineering, University of Essex, Colchester CO4 3SQ, UK*
[2]*BT Innovate & Design, pp. B29/OP8, Polaris House, BT Adastral Park, Ipswich IP5 3RE, UK*
**namaya@essex.ac.uk*

Abstract: An experimental demonstration of gridless spectrum and time switching is presented. We propose and demonstrate a bit-rate and modulation-format independent optical cross-connect architecture, based on gridless spectrum selective switch, 20-ms 3D-MEMS and 10-ns PLZT optical switches, that supports arbitrary spectrum allocation and transparent time multiplexing. The architecture is implemented in a four-node field-fiber-linked testbed to transport continuous RZ and NRZ data channels at 12.5, 42.7 and 170.8 Gb/s, and selectively groom sub-wavelength RZ channels at 42.7 Gb/s. We also showed that the architecture is dynamic and can be reconfigured to meet the routing requirements of the network traffic. Results show error-free operation with an end-to-end power penalty between 0.8 dB and 5 dB for all continuous and sub-wavelength channels.

OCIS codes: (060.1155) All-optical networks; (060.4510) Optical communications.

References and links

1. M. Jinno, H. Takara, B. Kozicki, Y. Tsukishima, Y. Sone, and S. Matsuoka, "Spectrum-efficient and scalable elastic optical path network: architecture, benefits, and enabling technologies," IEEE Commun. Mag. **47**(11), 66–73 (2009).
2. H. Takahara, B. Kozicki, Y. Sone, T. Tanaka, A. Watanabe, H. Hirano, K. Yonenaga, and M. Jinno, "Distance-adaptive super-wavelength routing in elastic optical path network (SLICE) with optical OFDM," ECOC 2010, Torino, Italy, 2010.
3. B. Kozicki, H. Takara, Y. Tsukishima, T. Yoshimatsu, K. Yonenaga, and M. Jinno, "Experimental demonstration of spectrum-sliced elastic optical path network (SLICE)," Opt. Express **18**(21), 22105–22118 (2010).
4. H. Furukawa, N. Wada, and T. Miyazaki, "640-Gbit/s (64-wavelength x 10-Gbit/s) wide-colored and phase-modulated optical packet switching and buffering without packet power compensation," in Optical Fiber Communication Conference, OSA Technical Digest (CD) (Optical Society of America, 2009), paper PDPD7.
5. N. Wada, S. Shinadad, H. Furukawa, "Modulation format free optical packet switching technology," ICTON, WeC1.5, 2010.
6. P. Winzer, "Beyond 100G ethernet," IEEE Commun. Mag. **48**(7), 26–30 (2010).
7. S. Gringeri, B. Basch, V. Shukla, R. Egorov, and T. J. Xia, "Flexible architectures for optical transport nodes and networks," IEEE Commun. Mag. **48**(7), 40–50 (2010).
8. D. Simeonidou, R. Nejabati, G. Zervas, D. Klonidis, A. Tzanakaki, and M. J. O'Mahony, "Dynamic optical network architectures and technologies for existing and emerging grid services," J. Lightwave Technol. **23**(10), 3347–3357 (2005).
9. Y. Qin, G. Zervas, V. Martini, M. Ghandour, M. Savi, F. Baroncelli, B. Martini, P. Castoldi, C. Raffaelli, M. Reed, D. Hunter, R. Nejabati, and D. Simeonidou, "Service-oriented multi-granular optical network testbed," in Optical Fiber Communication Conference, OSA Technical Digest (CD) (Optical Society of America, 2009), paper OWK2.
10. G. Zervas, L. Sadeghioon, Y. Qin, R. Nejabati, and D. Simeonidou, "Demonstration of novel multi-granular switch architecture on an application-aware end-to-end multi-bit rate OBS network testbed," ECOC 2007 PDP, PDS 3.2, Germany, September 2007.
11. L. Hui, M. Takagi, H. Imaizumi, and H. Morikawa, "Preliminary demonstration of hybrid optical switching node with dynamic wavelength resource allocation using SOA switch," OECC 2009, pp.1–2, 13–17 July (2009).
12. T. Miyazawa, H. Furukawa, K. Fujikawa, N. Wada, and H. Harai, "Partial implementation and experimental demonstration of an integrated optical path and packet node for new-generation networks," in Optical Fiber Communication Conference, OSA Technical Digest (CD) (Optical Society of America, 2010), paper OThP4.
13. M. Takagi, H. Li, K. Watabe, H. Imaizumi, T. Tanemura, Y. Nakano, and H. Morikawa, "400Gb/s hybrid optical switching demonstration combining multi-wavelength OPS and OCS with dynamic resource allocation," in Optical Fiber Communication Conference, OSA Technical Digest (CD) (Optical Society of America, 2009), paper OTuA6.

#145288 - $15.00 USD Received 4 Apr 2011; revised 7 May 2011; accepted 9 May 2011; published 24 May 2011

14. G. S. Zervas, M. De Leenheer, L. Sadeghioon, D. Klonidis, Y. Qin, R. Nejabati, D. Simeonidou, C. Develder, B. Dhoedt, and P. Demeester, "Multi-granular optical cross-connect: design, analysis and demonstration," J. Opt. Commun. Netw. **1**(1), 69–84 (2009).
15. N. Amaya, I. Muhammad, G. S. Zervas, R. Nejabati, D. Simeonidou, Y. Zhou, and A. Lord, "Experimental demonstration of a gridless multi-granular optical network supporting flexible spectrum switching," in Optical Fiber Communication Conference, OSA Technical Digest (CD) (Optical Society of America, 2011), paper OMW3.
16. M. C. Wu, O. Solgaard, and J. E. Ford, "Optical MEMS for lightwave communication," J. Lightwave Technol. **24**, 12 (2006).
17. K. Nashimoto, D. Kudzuma, and H. Han, "High-speed switching and filtering using PLZT waveguide devices," OECC 2010, Japan, July (2010).
18. G. Baxter, S. Frisken, D. Abakoumov, H. Zhou, I. Clarke, A. Bartos, and S. Poole, " Highly programmable wavelength selective switch based on liquid crystal on silicon switching elements," in Optical Fiber Communication Conference and Exposition and The National Fiber Optic Engineers Conference, Technical Digest (CD) (Optical Society of America, 2006), paper OTuF2.

1. Introduction

Wavelength Division Multiplexing (WDM) has become the standard core transmission technology in existing optical networks. In WDM, optical channels are confined to well-defined spectrum slots with either 50-GHz or 100-GHz spacing that have been standardized by the ITU. Hence, component manufacturers have been able to focus on producing devices at precise wavelengths, thereby providing technology compatibility and reducing development costs. However, there is a growing range of new technologies that require higher flexibility for allocating spectrum: bit-rate tunable transmitters that vary the number of sub-carriers in an orthogonal frequency division multiplex (OFDM) channel to achieve the required bit rate [1–3]; optical packet switching (OPS) systems that use several parallel wavelengths for packet transmission [4,5]; future 400 Gb/s and 1 Tb/s transmission that may require 75-GHz and 150-GHz channel spacing respectively [6,7].

Meanwhile, a broad range of emerging applications with widely varied traffic and dynamic bandwidth demands have motivated the development of networks that support not only circuits but also time-multiplex granularities in the optical domain [8–10]. Hybrid node architectures have been proposed for this purpose [11–13] but they often consist of a parallel arrangement of optical packet and circuit switches with limited flexibility and scalability. Other more flexible arrangements [14] do not support gridless or elastic operation i.e. dynamic allocation of optical spectrum according to channel requirements.

Recently we have demonstrated that flexible spectrum allocation has the potential to enable new arbitrary-bandwidth services and increase spectral efficiency for existing services [15]. In this paper we go beyond this work to propose and experimentally demonstrate a novel optical cross-connect architecture that supports flexible gridless switching and time domain multiplexing of arbitrary spectrum slices. The proposed architecture is implemented in a four-node network to selectively groom sub-wavelength data channels at 42.7 Gb/s and route continuous data traffic at 12.5 Gb/s, 42.7 Gb/s and 170.8 Gb/s with custom bandwidth allocation per channel.

2. Node architecture

The proposed node architecture is shown in Fig. 1(a). It comprises power splitters, high port-count slow optical switch (e.g. 20-ms-speed 3D micro-electro-mechanical systems (3D-MEMS) [16]), fast optical switches (e.g. 10-ns-speed PLZT (lead lanthanum zirconate titanate) [17]) and gridless Spectrum Selective Switch (SSS) (e.g. based on Liquid Crystal on Silicon (LCoS) [18]) arranged in a partial broadcast-and-select configuration. Incoming signals are replicated using the power splitters and input to the slow switch. Here, a resultant copy can be switched through the slow switch to an input of the SSS connected to the required output fiber link toward the next hop. The SSS is used to select, from the appropriate input, spectrum slices that contain the signals that require to be passed on to the output and block the remaining spectrum. In order to achieve this, transfer functions from each SSS input port to the common port are dynamically programmed. As shown in Figs. 1(b) and 1(c), each transfer function consists of one or several customized spectrum slices that can have arbitrary center

#145288 - $15.00 USD Received 4 Apr 2011; revised 7 May 2011; accepted 9 May 2011; published 24 May 2011

wavelength and bandwidth. Thus, multiple wavelengths or wavebands can be conveyed to the SSS output (Fig. 1(d)). Meanwhile, another copy of the input can be first passed through the slow switch and then through the fast switch to one of the SSS inputs. As copies of other input signals can also be connected to the same fast switch, it can groom data-units (Fig. 1(e)) that come from different sources and go towards the same destination using the same spectrum, provided they do not overlap in time. Then, the gridless SSS selects the spectrum slices that contain the aggregated channels and blocks all others on the same port. Sub-wavelength channels can be groomed by the fast switch or passed directly to the SSS without grooming. Therefore, this architecture supports allocation, space switching and time-multiplexing of arbitrary spectrum slices as shown in Fig. 1(f). Multicasting is also supported as replicas of an incoming signal can be connected to several gridless SSS, which can be configured to pass the same spectral range on to their respective outputs.

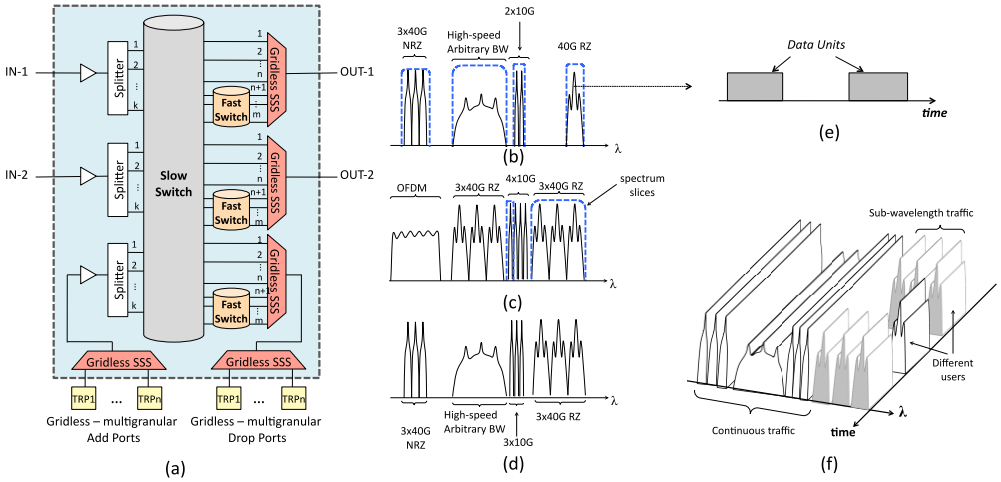

Fig. 1. (a) Gridless spectrum and time optical cross-connect architecture, (b) and (c) possible gridless SSS spectra of input ports, (d) gridless SSS output, (e) sub-wavelength channel data units, (f) gridless SSS output in time and λ.

3. Experimental setup

In the experimental demonstration of the proposed architecture we generated, transmitted, switched and received signals at several bit rates and modulation formats (listed in Table 1) using the gridless network testbed shown in Fig. 2.

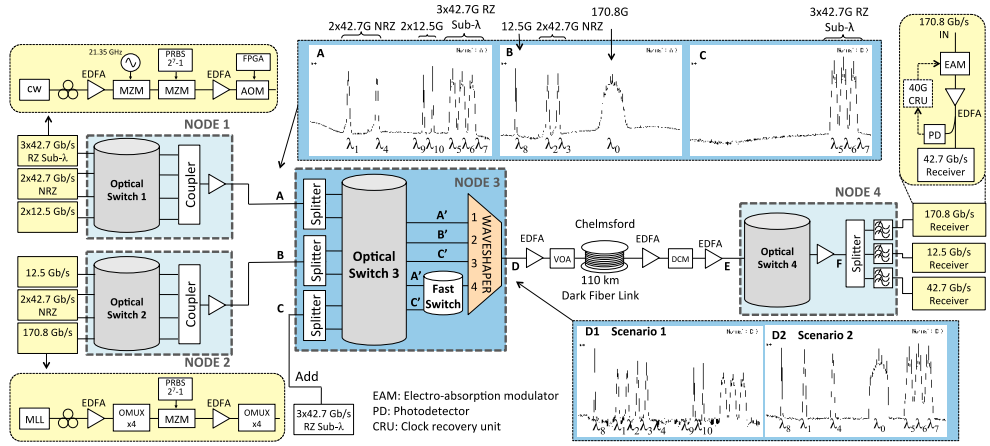

Fig. 2. Experimental setup and spectrum plot results.

#145288 - $15.00 USD Received 4 Apr 2011; revised 7 May 2011; accepted 9 May 2011; published 24 May 2011

The experimental testbed consists of a multi-format multi-bitrate transmitter, four optical nodes, 110-km field fiber link and receivers. At the transmitter, pulses at λ0 from a mode-locked laser (MLL) driven at 10.675 GHz are passed through a 4x optical multiplexer (OMUX), modulated with a pseudo-random bit sequence of length 2^7-1 (PRBS7) using a 40 GHz $LiNbO_3$ Mach-Zehnder modulator (MZM), amplified and input to a second 4xOMUX to produce a 170.8 Gb/s signal. Also, continuous 42.7 Gb/s NRZ signals are generated by modulating four continuous wave (CW) sources (λ1-λ4) with PRBS7 using a $LiNbO_3$ MZM. Sub-wavelength channels are generated from three CW sources (λ5-λ7) that are input to a $LiNbO_3$ MZM pulse carver and modulated with PRBS7 using a second $LiNbO_3$ MZM to produce continuous 42.7 Gb/s RZ signals. Then, these signals are combined and replicated using a 4x2 coupler and the two copies are input to two separate acousto-optic modulators (AOM) controlled by a field-programmable gate array (FPGA) to generate six channels carrying data-units of 9-μs duration followed by an 11-μs blank. Finally, a traffic analyzer generates two 12.5-Gb/s NRZ channels modulated with PRBS23, using two standard 10GE transponders. One of the channels (λ8) is used directly as input traffic to the network while the other is wavelength-converted using OEO technique to generate two 12.5 Gb/s NRZ wavelengths (λ9, λ10).

These signals have different spectrum and switching requirements. The 170.8 Gb/s RZ signal requires a bandwidth of 350 GHz, which would not be supported if the network conforms to a standard 100-GHz or 50-GHz grid. Additionally, the four 42.7 Gb/s NRZ signals have centre wavelengths 25 GHz off the ITU grid. The 42.7 Gb/s RZ channels carry non-continuous traffic and can be time-multiplexed with other non-continuous channels that use the same spectrum. Additionally, in order to demonstrate dynamic routing and all-optical arbitrary spectrum multiplexing two scenarios were implemented with different combinations of channels and switching requirements, as listed in Table 1.

Table 1. Generated Signals and Routing Requirements for Scenarios 1 and 2

	Source	Signal	Wavelength (nm)	Modulation	Bit Rate (Gbps)	Data
Scenario 1	Node 1	λ1, λ4	1538.39, 1543.14	NRZ	42.7	PRBS7
		λ5-1, λ6-1	1555.75, 1557.36	RZ	42.7 sub-λ	PRBS7
		λ9, λ10	1550.92, 1552.52	NRZ	12.5	PRBS23
	Node 2	λ2, λ3	1539.97, 1541.55	NRZ	42.7	PRBS7
		λ8	1534.64	NRZ	12.5	PRBS23
	Node 3	λ6-2, λ7-2	1557.36, 1558.98	RZ	42.7 sub-λ	PRBS7
Scenario 2	Node 1	λ1, λ4	1538.39, 1543.14	NRZ	42.7	PRBS7
		λ5-1, λ6-1, λ7-1	1555.75, 1557.36, 1558.98	RZ	42.7 sub-λ	PRBS7
		λ9, λ10	1550.92, 1552.52	NRZ	12.5	PRBS23
	Node 2	λ0	1550.52	RZ	170.8	PRBS7
		λ8	1534.64	NRZ	12.5	PRBS23
	Node 3	λ5-2, λ6-2, λ7-2	1555.75, 1557.36, 1558.98	RZ	42.7 sub-λ	PRBS7

In the experiment, signals added at Node 1 are switched through a 3D-MEMS-based optical switch (Optical Switch 1) and combined using a 4x1 coupler. Then, they are amplified using erbium doped fiber amplifier (EDFA) and transmitted to Node 3 over local fiber (Fig. 2 inset A). The same process is simultaneously performed with signals added to Node 2 (Fig. 2 inset B). At Node 3, local sub-wavelength channels are added at the same frequencies as the sub-wavelength channels coming from Node 1 (Fig. 2 inset C). Inputs to Node 3 coming from Node 1 (A), Node 2 (B) and local sub-wavelength channels (C) are replicated using 1x2 couplers and connected to the input ports of the 3D-MEMS Optical Switch 3. Here, cross-connections are created to switch each replica (A', B' and C') to an appropriate device port, depending on the routing requirements of the channels they contain. Thus, one of the A' replicas is sent to Gridless SSS port 1, which selects channels that go towards Node 4 and do not require all-optical time multiplexing. The other A' replica, together with C', are connected to the input ports of the 1x2 PLZT fast switch where sub-wavelength channels can be all-optically groomed in the time domain and subsequently selected by the Gridless SSS on its fourth port. C' is also connected to Gridless SSS port 3 where locally added channels may be

#145288 - $15.00 USD Received 4 Apr 2011; revised 7 May 2011; accepted 9 May 2011; published 24 May 2011

selected without passing through the PLZT switch for grooming. Selected signals are combined at the Gridless SSS common port (Fig. 2 insets D1 and D2) and transmitted to Node 4 over the 110 km of standard single mode fiber (SSMF) field-fiber link. Finally, at Node 4, channels are switched through 3D-MEMS Optical Switch 4, amplified, separated using band-pass filters (BPF) and fed to the receiver where their performance is measured.

4. Results

Table 1 specifies the signals switched through to Node 4 in each corresponding scenario and insets D1 and D2 in Fig. 2 show the output spectrum of Node 3 for scenarios 1 and 2 respectively. In the first scenario, according to the requirements of Table 1, five channels are selected on SSS port 1 (λ1, λ4, λ5-1, λ8, λ9), three on SSS port 2 (λ2, λ3, λ8) and one on SSS port 3 (λ7-2). Also, two sub-wavelength channels (λ6-1 and λ6-2) are all-optically groomed at the 1x2 PLZT 10-ns switch and subsequently selected on SSS port 4. The spectra of the signals transmitted from Node 1 (A'), Node 2 (B') and the local sub-wavelength channels added at Node 3 (C') are shown in Fig. 3(a1), 3(b1) and 3(c1) respectively. Replicas A' and C' input to the PLZT switch are shown in Fig. 3(d1) and 3(e1). Also, superimposed to the input spectra, and represented by the solid red line, there are the configured transfer functions of their respective SSS ports. The SSS output spectrum, shown in Fig. 3(f1), demonstrates that signals are successfully switched according to the requirements of the first scenario.

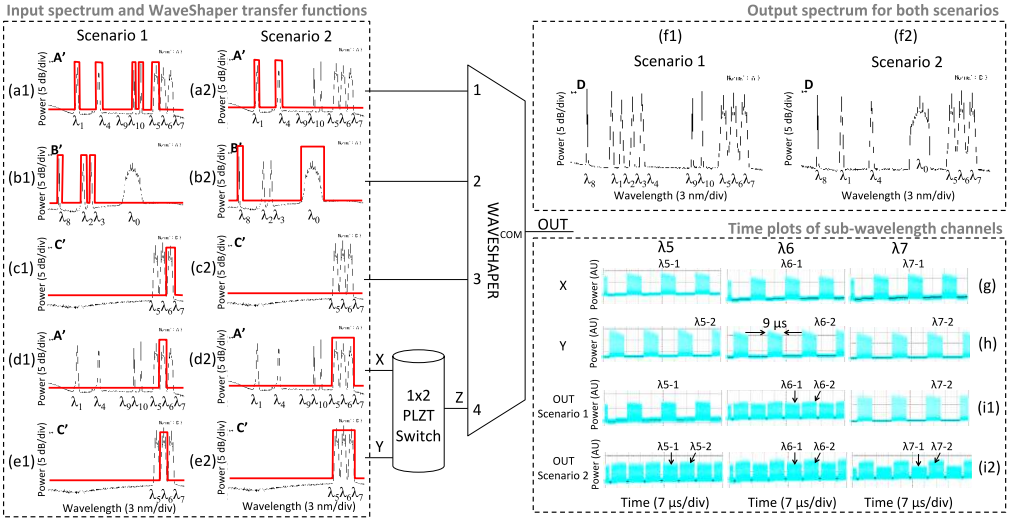

Fig. 3. Experimental results for scenarios 1 and 2.

Time plots of the sub-wavelength channels (at λ5-λ7) are also presented as seen at the PLZT switch inputs X (Fig. 3(g)) and Y (Fig. 3(h)) as well as at the SSS output (Fig. 3(i1)). Note that in Scenario 1 only λ6-1 and λ6-2 are groomed, since λ6 is the only wavelength selected on port 4 of the SSS. The other sub-wavelength channels are selected on different SSS ports, which are not connected to the PLZT switch. Thus, the SSS output includes at λ5 only λ5-1, from Node 1 (signal A') selected on Gridless SSS port 1; and at λ7 only λ7-2, added locally at Node 3 (C') and selected on port 3. Contention between the aggregated sub-wavelength channels (λ6-1 and λ6-2) is avoided by scheduling the transmission of data at the edge of the network. This process is performed by the FPGA that drives the AOMs for sub-wavelength channel generation. The mechanism adjusts the delay in the transmission of data-units taking into account the propagation time experienced by each sub-wavelength channel in order to avoid overlap when they arrive at the all-optical grooming node (Node 3).

Experimental results for the second scenario are also presented in Fig. 3(a2)–(f2). Here, transfer functions of the SSS ports have been configured to route signals according to the requirements for Scenario 2. For instance, the 170.8 Gb/s signal (λ0) is selected from Gridless

#145288 - $15.00 USD Received 4 Apr 2011; revised 7 May 2011; accepted 9 May 2011; published 24 May 2011

SSS port 2 (Fig. 3(b2)) whereas the two 12.5 Gb/s signals on port 1 that occupy the same spectral range (λ9 and λ10) are not selected (Fig. 3(a2)). Also, none of the sub-wavelength channels added locally (λ5-2, λ6-2 and λ7-2) are selected on port 3 as shown in Fig. 3(c2). Instead, the three wavelengths carrying sub-wavelength traffic (λ5, λ6 and λ7) are selected on SSS port 4 from the output of the PLZT switch where all-optical channel grooming takes place (Figs. 3(d2) and 3(e2)). Therefore, the three sub-wavelength channels coming from Node 1 (λ5-1, λ6-1, λ7-1 shown in Fig. 3(g)) and those added locally (λ5-2, λ6-2, λ7-2 shown in Fig. 3(h)) are simultaneously aggregated (Fig. 3(i2)). This functionality, termed sub-waveband granularity, may be used to provide larger bandwidths for bursty traffic.

Error free operation was confirmed on all channels through BER measurements. Results for the sub-wavelength 42.7 Gb/s RZ channels are shown in Fig. 4(a). Non-aggregated sub-wavelength channels had a power penalty measured at BER 10^{-9} of ~0.7 dB mainly due to the OSNR degradation from ASE noise introduced by the EDFAs in the links. The penalty introduced by Node 3 itself was negligible. As shown in Fig. 4(a), aggregated sub-wavelength channels show a ~3 dB degradation with respect to the case when they have not been aggregated. This is due to the lower energy per bit in aggregated channels for the same average channel power. Also, an additional penalty of ~1.5 dB was measured on the groomed λ7 due to the power difference of the aggregated channels at the output (Fig. 3(i2)). The performance of the 170.8 Gb/s channel was measured by de-multiplexing one of the four 42.7 Gb/s tributaries using an electro-absorption modulator (EAM) and feeding it to a 42.7 Gb/s receiver, as shown in Fig. 2. The end-to-end power penalty was 2.5 dB with 1.3 dB due to transmission over the field fiber link, as shown in Fig. 4(b). Higher penalties were observed for the NRZ channels; the 12.5-Gb/s end-to-end penalty was between 2.3 dB and 4.3 dB of which 2 to 3 dB were introduced over the field-fiber link. Finally, for the 42.7 Gb/s NRZ penalties ranging from 3.3 to 5.2 dB were measured with a contribution from the field-fiber link of 1.7 to 3.5 dB. The variation in penalty values introduced over the field-fiber link for the NRZ channels is mainly due to the different launch power of individual channels, as can be seen in Fig. 2 inset D1, and the tilted wavelength response of the EDFAs used in the link, which result in different OSNR and sensitivity values for each channel at the receiver.

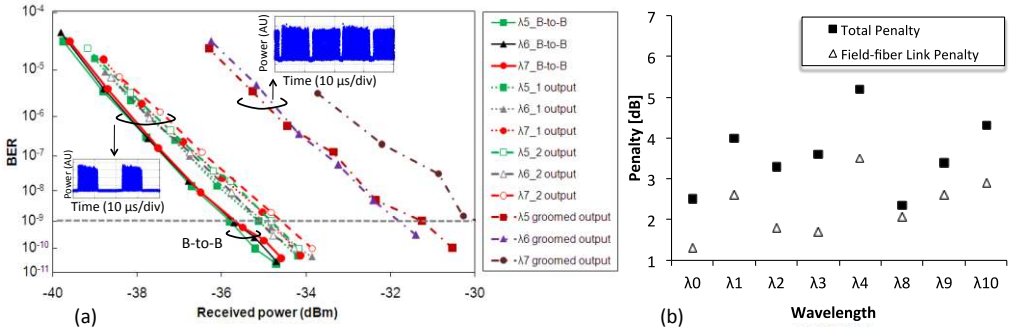

Fig. 4. (a) BER curves for sub-λ channels and (b) penalties for 170.8 Gb/s and NRZ channels.

5. Conclusion

We have proposed and experimentally demonstrated an architecture that supports allocation, space switching and time-multiplexing of arbitrary spectrum slices. We showed flexible routing of 12.5 Gb/s, 42.7 Gb/s and 170.8 Gb/s signals with customized gridless spectrum allocation and selective all-optical grooming of three 42.7 Gb/s sub-wavelength channels. Furthermore, we have shown that the architecture is dynamic and can be reconfigured according to the routing requirements of the input signals. We believe that the flexibility in allocating temporal and spectral resources provided by this architecture will enable a smooth optical network evolution for the introduction of future services and data rates.

#145288 - $15.00 USD Received 4 Apr 2011; revised 7 May 2011; accepted 9 May 2011; published 24 May 2011

Acknowledgments

This work has been supported by the EC FP7, grant agreement No. 247674, STRONGEST. We acknowledge Finisar for the WaveShaper and EpiPhotonics for the PLZT switch loan.

#145288 - $15.00 USD Received 4 Apr 2011; revised 7 May 2011; accepted 9 May 2011; published 24 May 2011